frontiers in Earth Science

ORIGINAL RESEARCH
published: 10 April 2018
doi: 10.3389/feart.2018.00025

Diversions of the Ribeira River Flow and Their Influence on Sediment Supply in the Cananeia-Iguape Estuarine-Lagoonal System (SE Brazil)

Flaminia Cornaggia[1]*, *Luigi Jovane*[1], *Luciano Alessandretti*[2†], *Paulo Alves de Lima Ferreira*[1], *Rubens C. Lopes Figueira*[1], *Daniel Rodelli*[1], *Gláucia Bueno Benedetti Berbel*[1] and *Elisabete S. Braga*[1]

[1] Instituto Oceanográfico, Universidade de São Paulo, São Paulo, Brazil, [2] Instituto de Geociências, Universidade de São Paulo, São Paulo, Brazil

OPEN ACCESS

Edited by:
Andrew C. Mitchell,
Aberystwyth University,
United Kingdom

Reviewed by:
Francois L. L. Muller,
Qatar University, Qatar
Ziming Yang,
Oakland University, United States

***Correspondence:**
Flaminia Cornaggia
flaminia.cornaggia@gmail.com

†Present Address:
Luciano Alessandretti,
Instituto de Geografia, Universidade Federal de Uberlândia, Uberlândia, Brazil

Specialty section:
This article was submitted to Geochemistry, a section of the journal Frontiers in Earth Science

Received: 23 November 2017
Accepted: 05 March 2018
Published: 10 April 2018

Citation:
Cornaggia F, Jovane L, Alessandretti L, Alves de Lima Ferreira P, Lopes Figueira RC, Rodelli D, Bueno Benedetti Berbel G and Braga ES (2018) Diversions of the Ribeira River Flow and Their Influence on Sediment Supply in the Cananeia-Iguape Estuarine-Lagoonal System (SE Brazil). Front. Earth Sci. 6:25. doi: 10.3389/feart.2018.00025

The Cananéia-Iguape system is a combined estuarine-lagoonal sedimentary system, located along the SE coast of Brazil. It consists of a network of channels and islands oriented mainly parallel to the coast. About 165 years ago, an artificial channel, the Valo Grande, was opened in the northern part of this system to connect a major river of the region, the Ribeira River, to the estuarine-lagoon complex. The Valo Grande was closed with a dam and re-opened twice between 1978 and 1995, when it was finally left open. These openings and closures of the Valo Grande had a significant influence on the Cananéia-Iguape system. In this study we present mineralogical, chemical, palaeomagnetic, and geochronological data from a sediment core collected at the southern end of the 50 km long lagoonal system showing how the phases of the opening and closure of the channel through time are expressed in the sedimentary record. Despite the homogeneity of the grain size and magnetic properties throughout the core, significant variations in the mineralogical composition showed the influence of the opening of the channel on the sediment supply. Less mature sediment, with lower quartz and halite and higher kaolinite, brucite, and franklinite, corresponded to periods when the Valo Grande was open. On the other hand, higher abundance of quartz and halite, as well as the disappearance of other detrital minerals, corresponded with periods of absence or closure of the channel, indicating a more sea-influenced depositional setting. This work represented an example of anthropogenic influence in a lagoonal-estuarine sedimentary system, which is a common context along the coast of Brazil.

Keywords: artificial channel, coastal system, sediment runoff, opening-closure dam, siltation, flooding, water salinity

INTRODUCTION

The Cananéia–Iguape estuarine-lagoonal system (**Figure 1**) is located in a large portion along the southern coast of the São Paulo State (Brazil), at latitude between 24°50′ and 25°40′ South and longitude between 47°20′ and 48°20′ West. This region is characterized by a group of four islands, separated by tide channels, coastal lagoons, little estuaries, and the Ribeira de Iguape River that

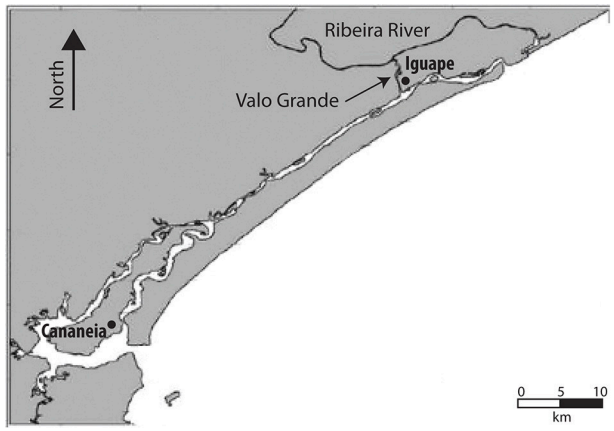

FIGURE 1 | Map of the Cananeia-Iguapé System.

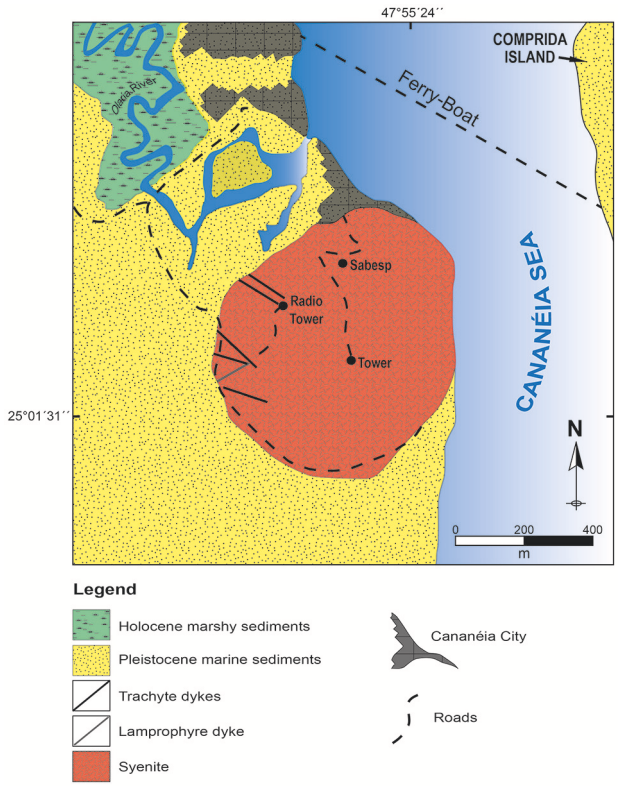

FIGURE 2 | Geologic map of the Cananéia Alkaline Massif area (adapted from Riccomini, 1995 with permission).

reaches the northern part of the hydrological system by the Valo Grande channel (Schaeffer-Novelli et al., 1990).

The Ribeira River has the largest drainage basin of the S-SE Brazilian coast (from 22°S to 30°S), with an area of about 25,000 km² (Bonetti Filho and de Miranda, 1997), with an annual average of 773.56 m^3/s (Bérgamo, 2000). The outflow of the Ribeira River is strongly influenced by the subtropical climate and in its lower course varies from about 300 to more than 1,200 m^3/s (Mahiques et al., 2009, 2013).

The bedrock of the Cananéia-Iguape Coastal Plain consists of a metamorphic basement of pre-Cambrian age. Different types of rock outcrop along the Ribeira River, such as quartzites, amphibolites, and green schists; intruded by granites, adamelites and granodiorites. Mesozoic intrusive alkaline rocks crosscut this basement complex and outcrop in various locations (Riccomini, 1995; de Souza et al., 1996). One of these outcrops forms the hill of São João (also called the Cananéia Alkaline Massif), in the municipality of Cananéia, which is the part of land closest to our core location. This hill is 137 m height and is surrounded by a coastal plain, filled with Pleistocene marine deposits (Cananéia Formation) and Holocene sediments of beach and mangrove swamp environments (see **Figure 2**) (Riccomini, 1995; Suguio et al., 2003).

The Valo Grande is a 4 km long artificial channel connecting the Ribeira River to the Cananéia-Iguape lagoon. It was excavated to facilitate the transportation of agricultural goods from the country lands to the harbor of Iguape city, between 1827 and 1852 (Geobrás and Fundacões, 1966; Mahiques et al., 2013). However, it began to be open to navigation in 1832 (Suguio and Petri, 1973). The channel was initially about 4.4 m wide and 2 m deep, but it quickly widened due to the high erosion produced by the strong stream. At the end of the XIX century, it was already wider than 100 m and deeper than 10 m (Geobrás and Fundacões, 1966).

According to da Silva Teles (1998), prior to the opening of the Valo Grande channel the river discharge was minimal in the lagoon, which was controlled mainly by tidal fluctuations and coastal currents. Since the opening of the Valo Grande, the coastal plain suffered drastic erosion, leading to a reduction of cultivable and inhabitable areas (Bérgamo, 2000; Mahiques et al., 2009). Consequently, a dramatic increase in sediment deposition occurred into the adjacent lagoonal setting, forming several new sediment bars, including the island of Iguape, and filled the port completely, making it inoperative by the late twentieth century (Teleginski, 1993). Moreover, changes in the fluvio-marine dynamics of the region introduced radical variations in temperature, salinity, currents, and water turbidity (Italiani and Mahiques, 2014).

In 1978, in response to the local people's request, the state government provided the construction of a dam to close the Valo Grande. This closure increased the salinity of the lagoon and caused a return of the seasonal flooding in the areas downstream the Valo Grande, which were occupied with crops at that time. Since then, major floods jeopardized the agricultural activities and the urban settlements of the region, until 1983, when the dam, already damaged by the floodings, was completely demolished by the local inhabitants. Subsequently, the dam was partially rebuilt but was unable to resist the continuous floodings and the sediment deposition. Therefore in 1995 it was completely demolished and, since then, the flux coming from the Ribeira river through the Valo Grande controls the geomorphological and ecological characteristics of the region (Italiani and Mahiques, 2014).

The various phases of opening and closure of the Valo Grande produced significant alteration of the sediment supply in the area

of Cananéia-Iguape. In this work we analyze bulk sedimentary mineral assemblages, sediment grain size, sediment magnetic properties, and pore water chemistry from a sediment core, which was collected in the lagoon near the southern connection to the sea, and from samples of the bedrock of the São Jõao Hill (also known as Cananéia Alkaline Massif), which represents the bedrock nearby the core site (Riccomini, 1995). The core was collected on the southern end of the lagoon, downstream to the main flow. This location receives sediment from all the different inputs into the sedimentary system and thus is ideal to assess the extension and the intensity of the disturbances created by the opening of the channel.

MATERIALS AND METHODS

The core CAN-N01 was collected using a gravity corer at −25.023831, −47.921750 in the Lagoon, south of the city of Cananéia. The core is 137 cm long with a 7.5 cm of diameter and was sampled each 2.5 cm.

Samples of the local bedrock, the Cananéia Alkaline Massif, forming the São João hill, were collected from an outcrop at −25.026223, −47.923203. The collection sites are shown in **Figure 3**.

All the measurements for this study were performed in the laboratories at the Institute of Oceanography of the University of São Paulo. The samples and parameters analyzed are listed below.

Grain Size

The samples were collected continuously along the core with 5 cm spacing. Carbonate constituents were removed with a 10% HCl solution in a beaker over a hot plate at 80°C, put inside an extraction hood while stirring hourly and adding more solution as it saturated. Afterwards, the samples were the washed at least twice, drained, and dried in an oven at a temperature of above 60°C for approximately 24 h.

Organic matter was removed with a 10% H-peroxide solution in a beaker over a hot plate, kept inside an extraction hood, at approximately 80°C, until the solution became colorless and changing the solution every 2 days. At the end, the samples were washed at least twice with distilled water, drained, and dried in an oven at a temperature of above 60°C for approximately 24 h. Grain sizes of 27 samples were determined using a Malvern Mastersizer-2000 Laser analyzer®.

Pore Waters

Pore water was extracted soon after core collection using Rizosphere® needles with diameter of 2.5 and a mean pore size of 0.15 μm to avoid fine sediment particles in pore waters. The extraction was performed in a regular interval distance of 10 cm. The water samples obtained (±10 mL) was fractionated and refrigerate to 4°C for dissolved nutrients (NH_4^+, PO_4^{3-} and $Si(OH)_4^-$) using colorimetric methods with a Biospectro® SP22 spectrophotometer. The analyses of nutrients were performed at the Laboratory of Biogeochemistry of Nutrients, Micronutrients and Traces in oceans (LABNUT-IOUSP). N-ammonium concentration was determined using Tréguer and Le Corre (1975) method with a detection limit of 0.02 μmol L^{-1} and a precision of ±0.01 μmol L^{-1}. Dissolved phosphate and silicate concentrations were determined using the recommendation of (Grasshoff, 1983) based on the molybdenum

FIGURE 3 | Location of sampled points. **(A)** CAN-N-01, **(B)** outcrop of São Jõao hill, Cananeia region. São Paulo, Brazil.

blue complex with a detection limit of 0.01 for phosphate and 0.1 μmol L^{-1} for silicate and a precision of ±0.01 and ±0.1 μmol L^{-1} respectively.

Paleomagnetism

In order to study in detail the magnetic properties of the core, a U-channel sample spanning the entire length of core (137 cm) was collected. Discrete oriented samples in cylindrical plastic boxes were also collected every 2.5 cm.

The U-channel was firstly used to study the natural remanent magnetization (NRM). To study the presence of primary and secondary magnetic components we applied an alternating field (AF) stepwise demagnetization, with steps of 0, 25, 50, 750, 100, 150, 20, 250, 300, 400, 500, 600, 700, 800, 900, and 1,000 mT. After each step, the u-channel was measured with a resolution of 1 cm using a 2G- Long Core Squid cryogenic magnetometer, located in a magnetically shielded room. The resultant curves were deconvoluted and analyzed using the software developed by Xuan and Channell (2009) and the principal component analysis of Kirschvink (1980), in order to isolate the characteristic remanent magnetization (ChRM).

Environmental Magnetism

Different rock magnetic measurements were performed to characterize the magnetic mineralogy of the core. Mass-dependent magnetic susceptibility was determined on discrete samples using an Agico KF1 Kappabridge.

Artificial magnetic fields of known characteristics were used in order to study the response of the samples in different conditions and the following parameters were determined: (a) anhysteretic remanent magnetization (ARM), which was measured first by imposing a 0.1 mT DC bias field while applying a 0.1 T demagnetizing alternating field, and then by progressively demagnetizing via AF with fields of 50, 100, 150, 200, 250, 300, 400, 500, 600, 700, 800, 900, 1,000 mT; (b) backfield isothermal remanent magnetization (BIRM), was imparted by applying first a 1.0T direct field (IRM@1.0) and subsequently by applying a 0.1 (IRM@-0.1) and 0.3 mT (IRM@-0.3) direct field in the opposite direction (e.g., King and Channell, 1991; Verosub and Roberts, 1995; Liu et al., 2012; Jovane et al., 2013).

From these parameters the S-ratios were calculated (S-Ratio300 as IRM@0.3/IRM@1.0; and S-Ratio100 as IRM@0.1/IRM@0.3), which measure the relative abundance of high coercivity (e.g., hematite, goethite) and low coercivity (e.g., magnetite) minerals. The hard isothermal remanent magnetization (HIRMs), which reflects the concentrations of high coercivity minerals, was calculated as (HIRM300 = (IRM@0.3+IRM@1.0)/2 and HIRM100= (IRM@0.1+IRM@1.0)/2); the relative magnetic grain size variations were estimated as ARM/IRM@1.0 (Evans and Heller, 2003). In order to perform the measurements with the 2G Cryogenic Magnetometer we used the Laboratory of Paleomagnetism of the Institute of Astronomy, Geophysics and Atmospheric Sciences of the University of São Paulo, Brazil.

Geochronology

A set of 11 samples for gamma spectrometry analysis were taken every 4 cm within the first 40 cm of the core, and then the material was prepared and analyzed following Figueira (2000) and Neves et al. (2014) recommendations. At first, the samples were lyophilized and homogenized, and 10 g were weighted and sealed in a container specific for gamma counting. After 21 days, the samples were counted in an EG&G ORTEC low-background gamma spectrometer (model GMX25190P, 1,79 keV FWHM for the ^{60}Co 1,33 MeV peak). An identical empty container was used to determine the background radiation of the detector and a source of ^{241}Am was used to determine the self-absorption factor of the samples. The samples were counted for 70,000 s and the photopeaks used in this analysis were 46.52 keV for ^{210}Pb, 609.31 keV for ^{226}Ra and 661.67 keV for ^{137}Cs. The quality control of this technique was assessed by measuring the same nuclides in certified reference materials (IAEA300, IAEA315, and IAEA326), and met all quality requirements, with statistical deviations and errors below 10%. Model CIC (Constant Initial Concentration) with unsupported ^{210}Pb (Robbins and Edgington, 1975) was used to measure the sedimentation and rates and to create an age model for the core.

Mineralogy

Approximately 1 cm^3 of sediment per sample was hand grinded in a jade mortar and then sieved through a 63 μm sieve. X-ray diffraction measurements were performed with an Olympus BTX II Benchtop X-ray Diffraction/X-ray Fluorescence device. The resulting X-ray diffraction data were processed using the Panalytical High Score Plus software, which includes the American Mineralogist Crystal Structure Database (AMSCD) and the Crystallography Open Database (COD). To determine the optimal number of expositions, diffractograms were obtained with different exposure times, and the best time/resolution was found at 100 exposures. Runs with more than 100 exposures did not yield significant improvement in mineral quantification, in agreement with Davis et al. (2015).

RESULTS

Grain Size

The results, presented using the Particle Size Distribution (PSZ) (**Figure 4**), showed high concentrations of fine and very fine sand (respectively on average 45.2 and 32.7%), with minor coarse sand, silt, and clay. No significant variations in grain size are observable throughout the core.

Pore Waters

The nutrients concentrations in pore waters are shown in **Figure 5**.

Concentration of N- ammonium ranged from 685 to 3,282 μmol L^{-1}. The values showed an increasing trend downcore, except from a value at 90 cm that decreased to 757 μmol L^{-1} (**Figure 5A**).

Phosphate concentration ranged from 104,6 to 291,7 μmol L^{-1}. The values showed an increasing trend downcore except at

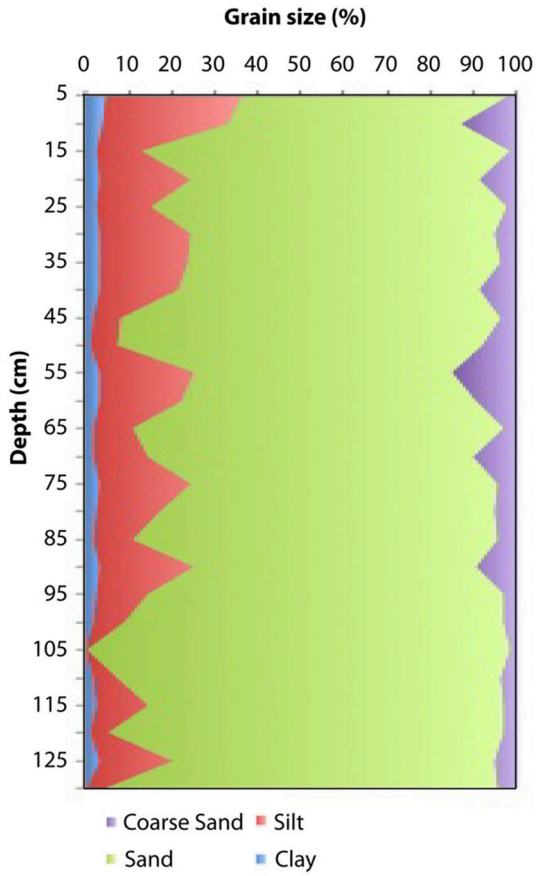

FIGURE 4 | Distribution of grain size in core CAN-N-01 profile.

20 cm that dropped from 170,3 to 104,6 μmol L^{-1}, and at 120 cm that dropped to 177,3 (**Figure 5B**).

Silicate values ranged from 640.2 to 836.2 μmol L^{-1}, with irregular distribution (**Figure 5C**).

Paleomagnetism

Magnetic Directions

Following the AF demagnetization process, the vast majority of the samples showed a particular pattern in the variation of intensity of the NRM, which decreased until 400 mT of AF, and then rose again, suggesting that the sample had acquired gyroremanence (GRM). The presence of an early gyroremanence precluded the study of the behavior of the sample at higher alternating fields.

The PCA analysis showed that the ChRM always had negative inclinations, as expected, with mean inclination of −37.2° (α_{95} of 1.6°), (**Figure 6**) that is perfectly in agreement with the expected value of −37.9° for the locality (as calculated with the Model WMM integrated between the years 2012 and 2014).

A secondary component was recognizable at low demagnetization fields, usually up to 100 mT, with lower inclinations, and was interpreted as a viscous remanent magnetization (VRM) carried by a very low-coercivity mineral.

Environmental Magnetism

The results of the environmental magnetic studies are summarized in **Figure 6**. The various parameters show little to no features, with almost constant values along the core. Relative concentration parameters, such as susceptibility, ARM are the most variable. A few positive peaks in NRM and ARM can be interpreted as an increase in the relative abundance of magnetic minerals, while negative peaks can be interpreted as a decrease

S-Ratios give information about the relative concentration of high and low (for S-Ratio300), and middle and low (S-Ratio100) coercivity minerals. The two curves have a similar behavior, with almost constant values close to 1 for the S-Ratio300 and 0.4 for the S-Ratio100 throughout the core. The variation along the core is minimal, with only a slight increase in the interval between 80 and 90 cm. The HIRMs curves also show almost no variation, with only some minor variations at 40 and 75 cm that should represent small fluctuations in the abundance of high coercivity minerals.

Geochronology

Model CIC was applied to the vertical profile of ^{210}Pb (**Figure 7**) and the calculated sedimentation rate was 0.43 ± 0.02 cm yr^{-1}. The exponential decay of ^{210}Pb ($r = 0.87$, $p < 0.05$; $\chi^2 = 0.44$, $p < 0.05$) shows that the sedimentation rate underwent little variations within the core. If any variation occurred, it was limited to the 8–12 cm of the core, and it is not statistically significant to the overall calculation, given the fit quality obtained from the statistical parameters presented above. Moreover, this result is supported by the vertical distribution of ^{137}Cs, which estimates a mean sedimentation rate of 0.39 ± 0.02 cm yr^{-1} for the first 40 cm of the core based on its horizon of maximum activity (corresponding to the nuclear fallout maximum of 1963 from past atomic tests).

The age model of the core was created, estimating a deposition year of 1920 for the 40-cm-deep layer of the core. Given that it was not observed evident changes in the sedimentation rate within the core, the age model created with the CIC model was extrapolated throughout the entire core.

X-Ray Diffraction

XRD analysis of the sediment core revealed three main mineralogical assemblages: (i) quartz around 99% and halite; (ii) quartz around 80%, and a minor fraction dominated by brucite; (iii) quartz between 60 and 80%, and a minor fraction dominated by kaolinite (**Figure 8**).

The interval from the top of the core to 65 cm depth is dominated by the mineralogical assemblages (ii) and (iii), with lower quartz content. Only a brief interval, between 15 and 22.5 cm, is dominated by the assemblage (i). Down-core, quartz content increases and below 95 cm it reaches the abundance of 97% or higher, with only halite as a minor mineral fraction. The XRD analysis of the bedrock samples yielded the results shown in **Table 1.**

Our results are in agreement with previous studies on the bedrock in this area, which found intrusive rocks, saturated or oversaturated in silica, with Na-feldspar more abundant than K-feldspar (Spinelli and Gomes, 2009).

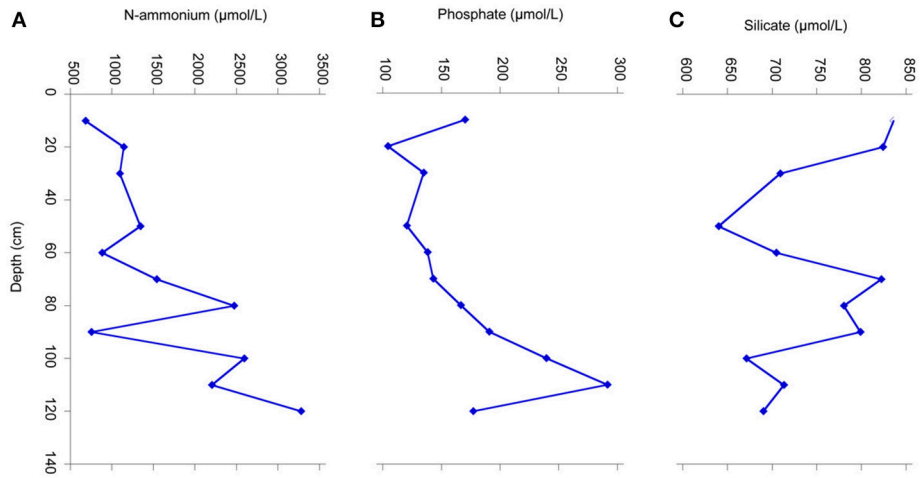

FIGURE 5 | Distribution profiles of dissolved nutrient concentrations in pore-waters: **(A)** N-Ammonium, **(B)** Phosphate, **(C)** Silicate for core CAN-N-01.

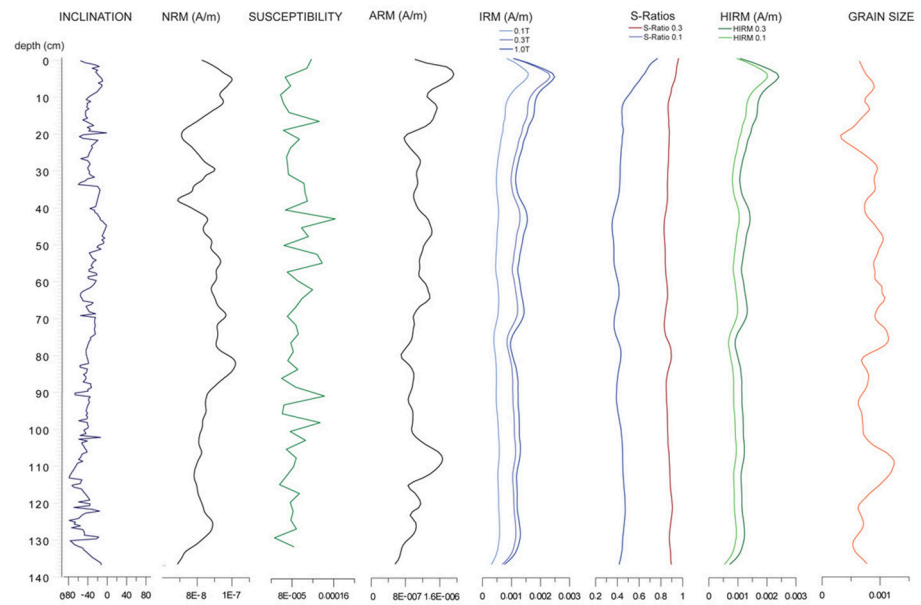

FIGURE 6 | Distribution of paleomagnetism data for core CAN-N-01.

DISCUSSION

The core was collected close to where the water outflows from the lagoon to the sea, in a moderate energy environment mainly controlled by the currents flowing parallel to the coast. In this context the lack of significant grain size variations along the core, indicates that the energy of the system remained constant during the deposition of the entire interval and therefore, the changes observed in the mineralogical assemblages must be related to the sediment supply, rather than to the depositional processes.

According to the age model of the core, the opening of the Valo Grande channel in 1852 should have occurred at 70 cm depth, its closure with the construction of the dam in 1978 at 16 cm, and the re-opening of the channel in 1983 at 13 cm.

The results of the environmental magnetic studies showed almost constant values along the core. The positive correlation between ARM and IRM peaks and the magnetic grain size suggested that the variation in concentration of magnetic minerals was accompanied by variations in the relative magnetic grain size, with a general trend of bigger grain size during periods of low concentration and vice-versa.

S-Ratio curves showed that the most predominant magnetic minerals are of low to middle coercivity, probably low-Ti magnetite (Ozima and Larson, 1970).

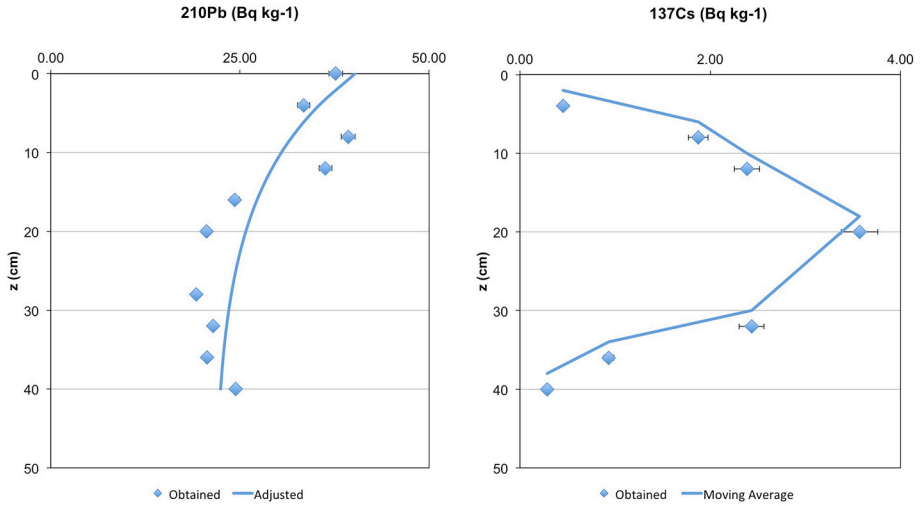

FIGURE 7 | Vertical distribution of ^{210xs}Pb and ^{137}Cs for core CAN-N-01.

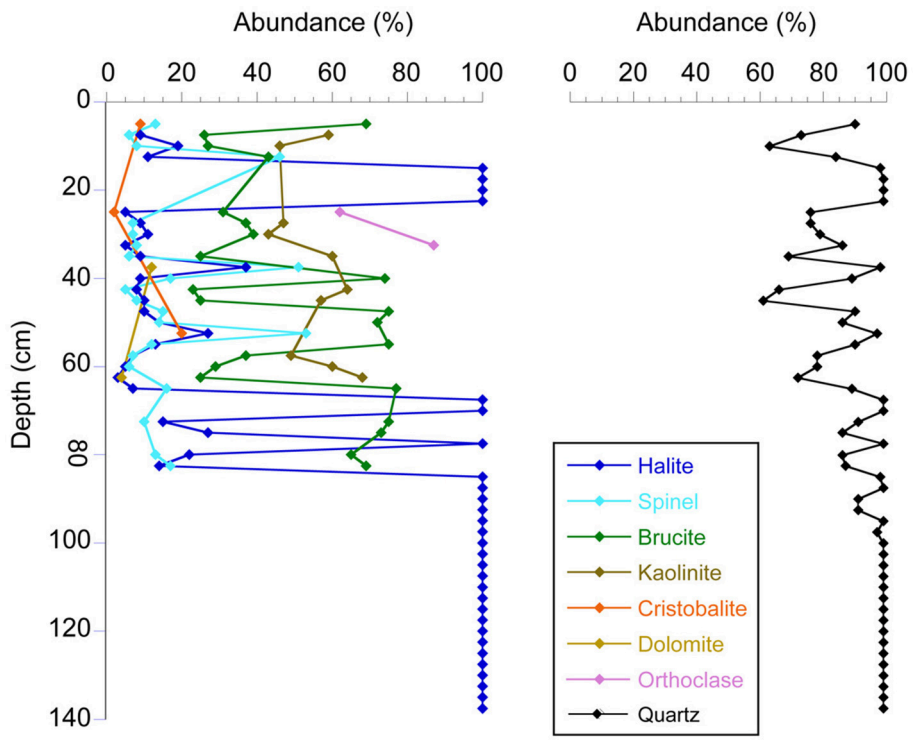

FIGURE 8 | Mineralogical distribution for core CAN-N-01: concentration of quartz on the right side and minor mineral fraction on the left side. Minor mineral abundances are expressed as normalized respect to quartz.

The peak at 5 cm found in the IRM, S-Ratios, and HIRMs curves could represent an increase of fine grained magnetite crystals in the sediment, comparable with the features found in sediments from Mamangua (RJ, Brazil), that were interpreted as the presence of living magnetotactic bacteria producing biogenic magnetite (Rodelli et al., in preparation).

Nutrients concentrations varied throughout the core despite the homogeneity of the grain size (**Figure 9**). This indicates fluctuations in redox conditions and in the amount of organic matter. The N-ammonium showed a minimum after the first opening the Valo Grande, and another one in the recent horizon, after the last opening. As N-ammonium is a product

of anaerobic destruction of organic matter its decreasing could be associated to organic matter decomposition in the presence of enough dissolved oxygen to allow the formation of nitrite and nitrate, which is corroborated by the increase of phosphate and silicate at this level. Phosphate also decreased from the opening of the Valo in 1852, contrary to N-ammonium, it increased toward the surface sediment in the uppermost layer. This could be the effect of the recent exploitation of phosphogypsum in the upland (Berbel et al., 2015). Silicate concentrations increased soon after the opening of the Valo Grande, signalizing an increase of silicate input. The increase of silicate is an excellent indicator of terrestrial and mineral inputs. In the recent horizon, silicate evidenced the increase of terrestrial input as demonstrated by phosphate, showing a return of the effective anthropogenic interference. For Braga et al. (2000), environments that have suffered from anthropogenic nutrients enrichment can be seriously modified and may present high levels of eutrophication. This can produce frequent and periodic low oxygenation in the water column, due to high nutrient supply and high primary production rate that consumes the oxygen (Gray et al., 2002; Smith and Demopoulos, 2003).

TABLE 1 | Mineralogical composition of the bedrock samples.

Sample	Albite (%)	Orthoclase (%)	Quartz (%)	Scapolite (%)
BR1	57	17	25	1
BR2	65	19	15	1
BR3	62	21	16	1
BR4	60	21	18	1
MEAN CONTENT	61	19,5	18,5	1

Mineralogical analyses show that halite and quartz have similar trends throughout the core, with maximum values corresponding to the periods when the Valo Grande channel was closed and decreasing when it was open (**Figure 9**). Their abundances have a marked increase between 15 and 22.5 cm, where the first type of mineralogical assemblage replaces the others. Apart from this interval, an alternation between the mineralogical assemblages (ii) and (iii) dominates from the top to the depth of 67.5 cm, where quartz content begins to increase and the first type of mineralogical assemblage becomes more frequent. Mineralogical assemblage (i) predominates from the depth of 90 cm down-core.

Halite can precipitate only from highly saline seawater, therefore its presence indicates the absence of riverine input that freshens the water. Our data suggest that, during the periods of absence or closure of the Valo Grande (between 1978 and 1983 and before 1827), the Ribeira River entered in the sea more northwards and did not supply significant amount of sediment to the Cananéia–Iguape aquatic environment.

The mineralogical composition of the sediment core indicates that during the time when the Valo Grande was opened, the sediments were characterized by lower quartz content and significant amounts of kaolinite, brucite, and franklinite, which corresponds also to a slight increase in detrital magnetite, estimated from environmental magnetic analyses. These minerals may have come from the alteration and erosion of the metamorphic basement forming most of the bedrock of the region and transported there by the opening of the Valo Grande. On the other hand, before the construction of the Valo Grande and during its closure, the sedimentary supply into the lagoon was controlled by sea currents, parallel to the coast, which delivered more mature sediments composed mainly by quartz. Our data shows that the sedimentary input into the lagoon changed during the last 165 years in response to the openings

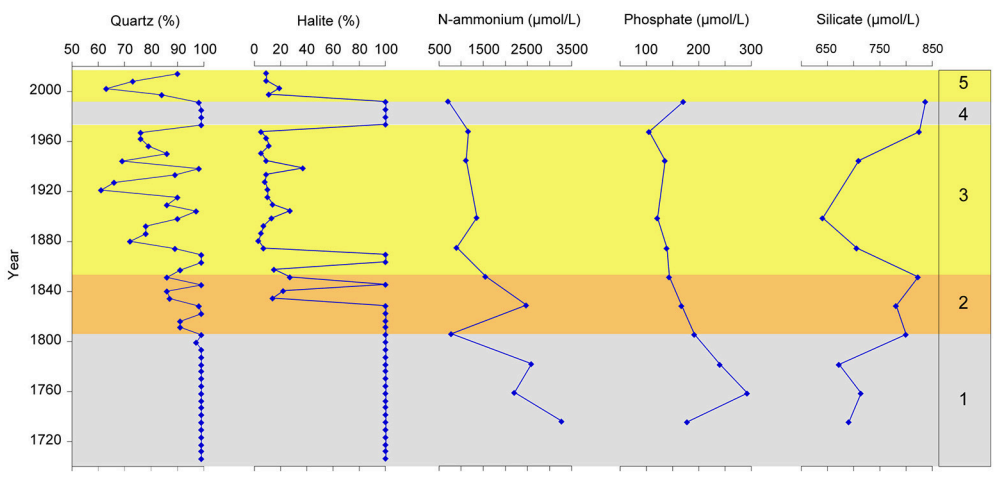

FIGURE 9 | Major mineral concentrations and pore water results over time for core CAN-N-01. Dating before 1850 has been extrapolated from the sedimentation rate. (1) Period before the construction of the Valo Grande channel; (2) Period during the construction of the Valo Grande channel; (3) Period during which the Valo Grande channel was completely open; (4) Period of the closure of the Valo Grande channel with a dam; (5) Period after the destruction of the dam and complete re-opening of the Valo Grande channel.

and closures of the Valo Grande channel. These variations are well displayed by the mineralogical assemblages, despite the homogenous grain size and environmental magnetic parameters.

CONCLUSIONS

Here, we presented detailed mineralogical, grain size, environmental magnetic, geochronological, and pore waters profiles of a sedimentary core from the southern portion of the estuarine-lagoonal system, near the Cananeia city. Despite the homogeneity of the grain size throughout the approximately 300 years interval, significant variations in the mineralogical composition of the non-quartz material revealed the influence of the opening of the channel on the sediment supply in the downstream part of the lagoon. A sediment composition presenting lower quartz and halite and higher kaolinite, brucite, and franklinite corresponded to periods of freshwater intrusion into the lagoon, due to the opening of the Valo Grande channel. High abundance of quartz and halite and the disappearance of the detrital minerals corresponded with prolonged periods of channel closure and a more sea-influenced setting, both before the opening of the Valo and during its following closures. These results are corroborated also by pore water dissolved nutrients. As estuarine-lagoonal sedimentary systems are rather common along the coast of Brazil, the case presented in this study could have several analogs in still less studied settings.

AUTHOR CONTRIBUTIONS

FC: Mineralogy, interpretation of the data and writing of the manuscript; LJ: Magnetic properties, Ph.D. supervisor, editing of the manuscript; LA: Grain size, editing of the manuscript; PA: Geochronology, editing of the manuscript; RL: Geochronology, editing of the manuscript; DR: Magnetic properties, editing of the manuscript; GB: Pore waters, editing of the manuscript; EB: Pore waters, editing of the manuscript.

FUNDING

Financial Support was provided by the Fundação de Amparo à Pesquisa do Estado de São Paulo, Grant 2011/22018-3, the CAPES/PROEX 0535/2017 Process n. 23038.006284/2017-72, the PhD program of the Instituto Oceanográfico da Universidade de São Paulo and the fellowship of Coordenação de Aperfeiçoamento de Pessoal de Nivel Superior.

REFERENCES

Berbel, G. B. B., Favaro, D. I. T., and Braga, E. S. (2015). Impact of harbour, industry and sewage on the phosphorus geochemistry of a subtropical estuary in Brazil. *Mar. Pollut. Bull.* 93, 44–52. doi: 10.1016/j.marpolbul.2015.02.016

Bérgamo, A. L. (2000). *Características da Hidrografia, Circulação e Transporte de sal: Barra de Cananéia, Sul do mar de Cananéia e Baía do Trapandé*. Ph.D. dissertation, Universidade de São Paulo.

Bonetti Filho, J., and de Miranda, L. B. (1997). Estimativa da descarga de água doce no sistema estuarino-lagunar de Cananéia-Iguape. *Rev. Bras. Oceanogr.* 45, 89–94.

Braga, E. S., Bonetti, C. V., Burone, L., and Bonetti Filho, J. (2000). Eutrophication and bacterial pollution caused by industrial and domestic wastes at the Baixada Santista Estuarine System–Brazil. *Mar. Pollut. Bull.* 40, 165–173. doi: 10.1016/S0025-326X(99)00199-X

da Silva Teles, A. P. S. (1998). *A evolução Geológica Quaternária ea Influência do Valo Grande na Dinâmica sEDIMENTAR da Área de Iguape*, São Paulo. Ph.D. dissertation.

Davis, B., Koch, A., Braun, G., O'Connor, C., Frost, E., Quinn, T., et al. (2015). "Wellsite Mineralogical Data Acquisition; Understanding Results from Multiple Analytical Sources," in *SPE European Formation Damage Conference and Exhibition. Society of Petroleum Engineers* (Budapest).

de Souza, L. A. P., Tessler, M. G., and Galli, V. L. (1996). O gráben de Cananéia. *Brazil. J. Geol.* 26, 139–150.

Evans, M. E., and Heller, F. (2003). *Environmental Magnetism: Principles and Applications of Enviromagnetics, Vol. 86*. Academic Press.

Figueira, R. C. L. (2000). *Inventory of Artificial Radionuclides in Seawater and Marine Sediments from Southern Coast of Brazil*. Ph.D. dissertation, Universidade de São Paulo, Library of the Brazilian Nuclear and Energy Research Institute (CNEN/IPEN), Sao Paulo, SP. Available online at: http://inis.iaea.org/search/search.aspx?orig_q=RN:37079223

Geobrás, S. A., and Fundacões, S. A. (1966). Complexo Valo Grande, mar Pequeno, rio Ribeira de Iguape. Relatório Geobrás. *S/A, Engenharia e Fundações para o Serviço do Vale o Ribeira do Departamento de Águas e Energia Elétrica, SP* 2.

Grasshoff, K., Ehrhardt, M., and Kremling, K. (1983). "Sampling techniques," in *Methods of Seawater Analysis* (Verlag Chemie), 1–19.

Gray, J. S., Wu, R. S. S., and Or, Y. Y. (2002). Effects of hypoxia and organic enrichment on the coastal marine environment. *Mar. Ecol. Prog. Ser.* 238, 249–279. doi: 10.3354/meps238249

Italiani, D. M., and Mahiques, M. M. (2014). O registro geológico da atividade antropogênica na região do Valo Grande, estado de São Paulo, Brasil. *Quat. Environ. Geosci.* 5. doi: 10.5380/abequa.v5i2.34522

Jovane, L., Herrero-Bervera, E., Hinnov, L. A., and Housen, B. A. (2013). Magnetic methods and the timing of geological processes. *Geol. Soc. Lond. Spec. Publ.* 373, 1–12 doi: 10.1144/SP373.17

King, J. W., and Channell, J. E. T. (1991). Sedimentary magnetism, environmental magnetism, and magnetostratigraphy. *Rev. Geophys.* 29, 358–370. doi: 10.1002/rog.1991.29.s1.358

Kirschvink, J. L. (1980). The least-squares line and plane and the analysis of palaeomagnetic data. *Geophys. J. Int.* 62, 699–718. doi: 10.1111/j.1365-246X.1980.tb02601.x

Liu, Q., Roberts, A. P., Larrasoaña, J., Banerjee, S. K., Guyodo, Y., Tauxe, L., et al (2012). Environmental magnetism: principles and applications. *Rev. Geophys.* 50:4. doi: 10.1029/2012RG000393

Mahiques, M. M., Burone, L., Figueira, R. C. L., Lavenére-Wanderley, A. A., Capellari, B., Rogacheski, C. E., et al. (2009). Anthropogenic influences in a lagoonal environment: a multiproxy approach at the valo grande mouth, Cananéia-Iguape system (SE Brazil). *Brazil. J. Oceanogr.* 57, 325–337. doi: 10.1590/S1679-87592009000400007

Mahiques, M. M., Figueira, R. C., Salaroli, A. B., Alves, D. P. V., and Gonçalves, C. (2013). 150 years of anthropogenic metal input in a Biosphere Reserve: the case study of the Cananéia–Iguape coastal system, Southeastern Brazil. *Environ. Earth Sci.* 68, 1073–1087. doi: 10.1007/s12665-012-1809-6

Neves, P. A., de Lima Ferreira, P. A., Bícego, M. C., and Figueira, R. C. L. (2014). Radioanalytical assessment of sedimentation rates in Guajará Bay (Amazon Estuary, N Brazil): a study with unsupported 210Pb and 137Cs modeling. *J. Radioanal. Nuclear Chem.* 299, 407–414. doi: 10.1007/s10967-013-2834-y

Ozima, M., and Larson, E. E. (1970). Low-and high-temperature oxidation of titanomagnetite in relation to irreversible changes in the magnetic properties of submarine basalts. *J. Geophys. Res.* 75, 1003–1017. doi: 10.1029/JB075i005p01003

Riccomini, C. (1995). Padrão de fraturamentos do maciço alcalino de Cananéia, Estado de São Paulo: relações com a tectônica mesozóico-cenozóica do sudeste do Brasil. *Revista Brasileira de Geociências* 25, 79–84.

Robbins, J. A., and Edgington, D. N. (1975). Determination of recent sedimentation rates in Lake Michigan using Pb-210 and Cs-137. *Geochim. Cosmochim. Acta* 39, 285–304. doi: 10.1016/0016-7037(75)90198-2

Schaeffer-Novelli, Y., Mesquita, H. D. S. L., and Cintrón-Molero, G. (1990). The Cananéia lagoon estuarine system, São Paulo, Brazil. *Estuaries Coasts* 13, 193–203. doi: 10.2307/1351589

Smith, C. R., and Demopoulos, A.W. J. (2003). "Ecology of the deep Pacific Ocean floor," in *Ecosystems of the World, Vol. 28, Ecosystems of the Deep Ocean*, ed P. A. Tyler (Amsterdam: Elsevier), 179–218.

Spinelli, F. P., and Gomes, C. D. B. (2009). A ocorrência alcalina de Cananeia, litoral sul do estado de São Paulo: química mineral. *Geologia USP. Série Científica* 9, 1–13. doi: 10.5327/Z1519-874X2009000100001

Suguio, K., and Petri, S. (1973). Stratigraphy of the Iguapé-Cananéia lagoonal region sedimentary deposits, São Paulo State, Brazil: part I: field observations and grain size analysis. *Boletim IG* 4, 01–20.

Suguio, K., Tatumi, S. H., Kowata, E. A., Munita, C. S., and Paiva, R. P. (2003). Upper Pleistocene deposits of the Comprida Island (São Paulo State) dated by thermoluminescence method. *Anais da Academia Brasileira de Ciências* 75, 91–96. doi: 10.1590/S0001-37652003000100010

Teleginski, A. (1993). Aspectos históricos e fundiários no Vale do Ribeira e sua influência no desenvolvimento econômico da região. *III Simpósio de Ecossistemas da Costa Brasileira* 1, 104–106.

Tréguer, P., and Le Corre, P. (1975). "Analyse des sels nutritifs sur autoanalyzer II. Methods," in *Manuel D'Analyse des Sels Nutritifs dans L'Eau de Mer*, Richards et Kletsh (modifiée) (Brest: Université de Bretagne Occidentale), 50–61.

Verosub, K. L., and Roberts, A. P. (1995). Environmental magnetism: past, present, and future. *J. Geophys. Res. Solid Earth* 100, 2175–2192.

Xuan, C., and Channell, J. E. T. (2009). UPmag: MATLAB software for viewing and processing u channel or other pass-through paleomagnetic data. *Geochem. Geophys. Geosyst.* 10:Q10Y07. doi: 10.1029/2009GC002584

Conflict of Interest Statement: The authors declare that the research was conducted in the absence of any commercial or financial relationships that could be construed as a potential conflict of interest.